Crystallization Tendency of Active Pharmaceutical Ingredients Following Rapid Solvent Evaporation—Classification and Comparison with Crystallization Tendency from Undercooled Melts

BERNARD VAN EERDENBRUGH, JARED A. BAIRD, LYNNE S. TAYLOR

Department of Industrial and Physical Pharmacy, School of Pharmacy and Pharmaceutical Sciences, Purdue University, 575 Stadium Mall Drive, West Lafayette, Indiana 47907

Received 18 February 2010; revised 13 April 2010; accepted 14 April 2010

Published online 8 June 2010 in Wiley InterScience (www.interscience.wiley.com). DOI 10.1002/jps.22214

ABSTRACT: In this study, the crystallization behavior of a variety of compounds was studied following rapid solvent evaporation using spin coating. Initial screening to determine model compound suitability was performed using a structurally diverse set of 51 compounds in three different solvent systems [dichloromethane (DCM), a 1:1 (w/w) dichloromethane/ethanol mixture (MIX), and ethanol (EtOH)]. Of this starting set of 153 drug–solvent combinations, 93 (40 compounds) were selected for further evaluation based on solubility, chemical solution stability, and processability criteria. These systems were spin coated and their crystallization was monitored using polarized light microscopy (7 days, dry conditions). The crystallization behavior of the samples could be classified as rapid (Class I: 39 cases), intermediate (Class II: 23 cases), or slow (Class III: 31 cases). The solvent system employed influenced the classification outcome for only four of the compounds. The various compounds showed very diverse crystallization behavior. Upon comparison of classification results with those of a previous study, where cooling from the melt was used as a preparation technique[1], a good similarity was found whereby 68% of the cases were identically classified. Multivariate analysis was performed using a set of relevant physicochemical compound characteristics. It was found that a number of these parameters tended to differ between the different classes. These could be further interpreted in terms of the nature of the crystallization process. Additional multivariate analysis on the separate classes of compounds indicated some potential in predicting the crystallization tendency of a given compound.
© 2010 Wiley-Liss, Inc. and the American Pharmacists Association J Pharm Sci 99:3826–3838, 2010
Keywords: crystallization; amorphous state; spin coating; solvent evaporation; classification; physical stability

INTRODUCTION

The current drug discovery process is characterized by an increase in new chemical entities which can be classified as Class II and Class IV compounds, according to the Biopharmaceutical Classification System[2] (BCS). Hence, bioavailability of these compounds is limited due to a low aqueous solubility and, in some cases, also permeability. To enhance bioavailability, a number of formulation platforms have been introduced, such as particle size reduction,[3] complexation,[4] the use of cosolvents,[5] chemical derivatization using prodrug strategies,[6] and rendering the drug amorphous, often through the formation of a solid dispersion.[7] The interest in the latter strategy originates from the higher (apparent) solubility of the amorphous form compared to the crystalline counterpart(s). Calculations based on thermodynamic parameters suggest relative increases in solubility up to 1600-fold, although the extent of the theoretical enhancement is highly compound specific.[8] Furthermore, crystallization often drastically reduces any potential solubility advantage; crystallization can occur both during storage of the solid[9–11] and upon dissolution of the amorphous solid.[12–14]

Crystallization during storage of amorphous pharmaceuticals has recently been reviewed.[15] The authors highlighted that crystallization from the amorphous state is a complex phenomenon, making an overall understanding of the crystallization behavior of

Supporting Information may be found in the online version of this article.

Correspondence to: Lynne S. Taylor (Telephone: +1-765-496-6614; Fax: +1-765-494-6545; E-mail: lstaylor@purdue.edu)

Journal of Pharmaceutical Sciences, Vol. 99, 3826–3838 (2010)
© 2010 Wiley-Liss, Inc. and the American Pharmacists Association

WILEY InterScience® DISCOVER SOMETHING GREAT

amorphous drugs an ambitious goal. As crystallization is the combined result of nucleation and crystal growth, all factors affecting one or both processes can be expected to have an effect on the overall crystallization behavior. Factors known to have an effect on crystallization from the amorphous state are thermodynamic [e.g., the free energy difference between the crystalline and amorphous states (ΔG_v)], kinetic [e.g., molecular mobility, for which the glass transition temperature (T_g) is often used as an indicator], or molecular [e.g., hydrogen bonding interactions] in nature. Furthermore, factors such as moisture content and the method employed for generation of the amorphous form have also been reported to influence crystallization behavior[15] (and references therein).

Possible routes for the generation of amorphous materials are cooling from the melt, condensation from the vapor state, mechanical disruption of the crystal lattice, precipitation from solution and solvent evaporation.[15,16] From the perspective of industrial production, however, it is pertinent to mention that amorphous drugs and formulations are conventionally prepared either by cooling from the melt (e.g., melt extrusion) or by solvent evaporation/sublimation (e.g., spray drying or freeze-drying).[17]

There are numerous examples in the literature describing the stability and/or stabilization of amorphous pharmaceuticals.[18–20] Typically, the crystallization behavior of only one or a few compounds is reported in such studies. The crystallization behavior of a larger data set of compounds is seldom evaluated although this approach would potentially yield a more general understanding of the crystallization of pharmaceuticals, in particular if the crystallization conditions are standardized. A recent example of this approach is provided in the study by Greaser et al.,[21] where the authors attempted to correlate the amorphous stability of 12 active pharmaceutical ingredients (APIs) with a number of kinetic and thermodynamic parameters. Samples were prepared *in situ* in a differential scanning calorimeter (DSC) by cooling from the melt in DSC pans. Although a reasonable correlation could be observed between the physical stability above the glass transition temperature (T_g) and the configurational entropy, the authors concluded that: "*. . . when dealing with the amorphous state, complex kinetic and thermodynamic processes have to be considered and no simple straightforward attempt will suffice to characterize physical stability . . .*" Furthermore, multivariate analysis was suggested to be a potentially better approach, given the complexity of crystallization. In a recent study, the glass forming ability and glass stability of a set of 51 structurally diverse compounds was investigated and classified.[1] In common with the Greaser study, samples were prepared by cooling from the melt in DSC pans. Multivariate analysis was utilized to probe important compound properties that correlated with the crystallization tendency.

Although solvent evaporation techniques are commonly used to produce amorphous materials, there are fewer studies evaluating the crystallization tendency of APIs produced using this method. Furthermore, it is of interest to evaluate if there are similarities between the crystallization tendency from the melt and following solvent evaporation, in other words, how much does the method of preparation affect the crystallization tendency versus the inherent properties of the compound? The aim of the current study was thus to investigate the crystallization behavior of a large group of compounds following rapid solvent evaporation and to compare the results to the melt crystallization behavior. Fifty-one model compounds, for which the melt crystallization behavior has been determined, were evaluated. Three different solvent systems having different polarities were selected [dichloromethane (DCM), a 1:1 (w/w) dichloromethane/ethanol mixture (MIX), and ethanol (EtOH)] and rapid solvent evaporation was performed by spin coating, enabling the formation of thin films using milligram quantities of drug. The short-term physical stability of the resultant films was monitored using polarized light microscopy. The observed crystallization behavior following spin coating was then classified into three classes: "Class I": rapid crystallization; "Class II": intermediate crystallization; "Class III": slow crystallization and compared to the melt crystallization behavior, Principal component analysis (PCA) was performed using a set of physicochemical compound characteristics in order to provide insight into the origin of the differences in crystallization behavior.

MATERIALS AND METHODS

Materials

Atenolol, benzocaine, dibucaine, lidocaine, miconazole, procaine, and tolbutamide were obtained commercially from Spectrum Chemical (Gardena, CA). Aceclofenac, clarithromycin, and loratadine were obtained commercially from Attix Pharmachem (Toronto, ON, Canada). 4-biphenylcarboxylic acid, 4-biphenylmethanol, 4-biphenylcarboxaldehyde, 4-phenylphenol, acetaminophen, anthranilic acid, antipyrin, benzamide, bifonazole, anhydrous caffeine, chlorpropamide, chlorzoxazone, cinnarizine, clofoctol, clotrimazole, droperidol, felbinac (4-biphenylacetic acid), fenofibrate, flufenamic acid, flurbiprofen, haloperidol, indomethacin, indoprofen, ketoprofen, niclosamide, nilutamide, nimesulide, PABA (4-aminobenzoic acid), phenacetin (*p*-acetophenetidide), pimozide, probucol, D-(−)-salicin, tolazamide, and

tolfenamic acid were purchased from Sigma–Aldrich, Inc. (St. Louis, MO). Anhydrous theophylline was obtained commercially from Ruger Chemical Co. (Irvington, NJ). Carbamazepine, griseofulvin, itraconazole, ketoconazole, nifedipine, and piroxicam were bought from Hawkins, Inc. (Minneapolis, MN). Ibuprofen was obtained commercially from Albemarle Co. (Baton Rouge, LA). Dichloromethane (ChromAR®), methyl alcohol (anhydrous, ChromAR®), phosphorous pentoxide (powder), and potassium nitrate (crystal) were purchased from Mallinckrodt Baker, Inc. (Phillipsburg, NJ). Ethyl alcohol (200 proof) was purchased from Pharmco Products, Inc. (Brookfield, CT) and Aaper (Shelbyville, KY). Trifluoroacetic acid was commercially obtained from Acros Organics (Geel, Belgium). Felodipine was a generous gift from AstraZeneca (Södertälje, Sweden). Ritonavir was kindly provided from the Clinton Foundation (New York, NY). Celecoxib was kindly provided by Pfizer, Inc. (Groton, CT).

Determination of the Optimal Drug Concentration for Spin Coating

To optimize the solution concentration for spin coating, the average film thickness of spin-coated felodipine films was determined as a function of concentration in DCM, MIX, and EtOH. Felodipine solutions of 0.03, 0.07, 0.13, 0.20, 0.26, 0.52, 0.78, 1.04, and 1.30 M were prepared in the different solvents (only solutions up to 0.26 M could be prepared in EtOH due to the lower solubility of felodipine in this solvent). Subsequently, spin coating was performed as described below. Following spin coating, the average film thickness was estimated from the weight gain of the glass substrate, using a value of 1.28 g/mL for the density of amorphous felodipine.[22] Sample flatness was evaluated visually and the appearance of crystals in the bulk of the films was examined using polarized light microscopy. Finally, samples were stored for 2 days in a closed container at high relative humidity (room temperature, relative humidity of 94%, saturated KNO_3 solution), to convert the amorphous film into a crystalline product.

Determination of Drug Solubility and Degradation in the Solvent Systems

The solubility of the drugs in DCM, MIX, and EtOH was determined using UV spectroscopy. Measurements were performed using a UV–Visible spectrophotometer (Cary 300 Bio; Varian, Inc., Palo Alto, CA), in double beam mode. Quartz cuvettes (10 mm pathlength; Starna Cells, Inc., Atascadero, CA) were used and the average of five replicate absorbance measurements (1 s) was determined. Standards were prepared at concentrations of 0 (blank), 10%, 25%, 40%, 60%, 80%, and 100% of the highest standard concentration used. All absorbances measured were $\leq$1.5 AU, to ensure linearity of the calibration curves. The wavelengths used for detection, solvents used for preparation of the calibration curve standards, and the correlation coefficients of the calibration curves are summarized in Table 1.

Samples were prepared by adding an excess of drug compound to a 1.5 mL Eppendorf tube (Eppendorf, Hamburg, Germany) containing 1 mL of solvent. After 24 h of equilibration at room temperature on an orbit shaking platform (VWR minishaker; VWR International, LLC, West Chester, PA), the saturated solutions were separated from the undissolved drug using centrifugation (16,000*g*, 10 min), using an Eppendorf 4515C centrifuge equipped with a F-45-18-11 rotor (Eppendorf). In cases where centrifugation was impossible, due to poor separation efficiency (DCM has a density of 1.325 g/mL, close to or higher than that of a number of drug compounds), filtration was performed using a glass syringe (GASTIGHT® #1010; Hamilton Co., Reno, ND) and 0.2 μm PTFE syringe filters (13 mm; VWR International, LLC). After isolation of the supernatant, samples were diluted into the range of the calibration curves, using the same solvent as for preparation of the standards, and their absorbance was measured. Each experiment was performed in triplicate and the average and standard deviations were calculated.

After solubility determination, drug degradation in the supernatant was assessed using HPLC-UV. The instrument used was an HP1000 system, consisting of a G1322A degasser, a G11312A binary pump, a G1313A auto sampler, and a G1314A variable wavelength detector (Hewlett-Packard GmbH, Waldbronn, Germany). A 15.0 cm, 4.6 mm, 5 μm Supelcosil™ ABZ+Plus column (Supelco, Bellefonte, PA) was used and the mobile phase consisted of an aqueous phase of 0.1% trifluoroacetic acid in water and methanol as the organic phase. A gradient method was applied using 90:10 (v/v) aqueous/organic during the first 2 min, followed by linear transition to 10:90 (v/v) aqueous/organic from 2 to 14 min, after which the solvent composition was kept constant. The flow rate was 1 mL/min, the injection volume was 2 μL, and detection was carried out at 230 nm. Samples were diluted in methanol prior to injection. The resulting chromatograms were compared to those of freshly prepared solutions of the drugs in methanol.

Spin Coating and Solidification by Slow Solvent Evaporation

Spin coating was performed using a KW-4A spin coater (Chemat Technology, Inc., Northridge, CA) on 18 mm × 18 mm microscope cover slips (Corning Incorporated, Corning, NY). Briefly, 200 μL of drug solution was spread out over the cover slip. Subse-

Table 1. Compounds Used in This Study, With Information Relevant to Solubility Determination: Solvents Used for Standard and Sample Preparation, Detection Wavelengths, and Correlation Coefficients of the Calibration Curves

Compound	Solvent	λ (nm)	R^2
4-Biphenylcarboxaldehyde	MeOH	286	0.998
4-Biphenylcarboxylic acid	MeOH	268	1.000
4-Biphenylmethanol	MeOH	252	0.999
4-Phenylphenol	MeOH	261	0.999
Aceclofenac	MeOH	275	0.999
Acetaminophen	MeOH	248	0.999
Anthranilic acid	MeOH	335	1.000
Antipyrin	MeOH	267	0.999
Atenolol	MeOH	275	1.000
Benzamide	MeOH	265	1.000
Benzocaine	MeOH	292	1.000
Bifonazole	EtOH	254	1.000
Caffeine	MeOH	272	0.999
Carbamazepine	MeOH	285	1.000
Celecoxib	MeOH	252	1.000
Chlorpropamide	MeOH	265	0.999
Chlorzoxazone	MeOH	282	1.000
Cinnarizine	MeOH	250	1.000
Clarithromycin	MeOH	215	1.000
Clofoctol	MeOH	281	1.000
Clotrimazole	EtOH	261	1.000
D-(−)-Salicin	MeOH	268	0.999
Dibucaine	MeOH	327	0.999
Droperidol	MeOH	281	1.000
Felbinac	MeOH	252	1.000
Felodipine	MeOH	360	1.000
Fenofibrate	MeOH	286	1.000
Flufenamic acid	MeOH	291	0.999
Flurbiprofen	ACN	247	1.000
Griseofulvin	MeOH	291	1.000
Haloperidol	MeOH	242	1.000
Ibuprofen	MeOH	258	1.000
Indomethacin	MeOH	318	1.000
Indoprofen	MeOH	282	1.000
Itraconazole	DCM	262	1.000
Ketoconazole	MeOH	296	1.000
Ketoprofen	MeOH	255	0.999
Lidocaine	MeOH	262	1.000
Loratadine	MeOH	247	1.000
Miconazole	MeOH	265	0.999
Nifedipine	MeOH	340	1.000
Nilutamide	MeOH	265	1.000
Nimesulide	MeOH	298	1.000
PABA	MeOH	288	0.999
Phenacetin	MeOH	249	1.000
Pimozide	MeOH	281	0.999
Piroxicam	MeOH	340	1.000
Probucol	MeOH	242	1.000
Procaine	MeOH	294	1.000
Ritonavir	MeOH	239	0.999
Theophylline	MeOH	270	1.000
Tolazamide	MeOH	256	0.999
Tolbutamide	MeOH	257	1.000
Tolfenamic acid	MeOH	289	1.000

MeOH, methanol; EtOH, ethanol; ACN, acetonitrile; DCM, dichloromethane.

quently, the sample was spun for 20 s at 8000 rpm. Each solution was spin coated in triplicate.

For the samples classified as "Class III" (see the Evaluation and Classification of Crystallization Behavior on Storage Section), additional samples were prepared at slower evaporation rates. For these experiments, 400 μL of drug solution was transferred into a cylindrical glass crystallization vessel (12 mm diameter × 6 mm height) and solvent evaporation was performed at ambient conditions. Each experiment was performed in triplicate.

Evaluation and Classification of Crystallization Behavior upon Storage

Crystallization of the samples immediately after spin coating and upon storage was evaluated with polarized light microscopy using an Eclipse E600 POL polarizing microscope (Nikon Corporation, Tokyo, Japan), equipped with 4×, 10×, 20×, and 40× objectives. Crystallinity of the three replicates prepared for each drug–solvent combination was evaluated visually, based on the extent of the observed birefringence. As the spin-coated films are very thin (about 1 μm), it is reasonable to assume that when crystallization occurs, it will do so over the complete height of the film. Hence, this two-dimensional analysis enables a semi-quantitative evaluation of crystallinity based on the relative areas of crystalline and amorphous regions.

Spin-coated samples were evaluated for crystallization within 30 min after spin coating ("day 0" time point). Subsequently, samples were stored overnight under vacuum to remove residual solvent, followed by evaluation ("day 1"). For some compounds, applying a vacuum resulted in sublimation of the film. Therefore, unless crystallization was complete prior to storage under vacuum, compounds showing this behavior (antipyrin and ibuprofen) were excluded from the screening. Samples were subsequently placed in a container under dry conditions, using P_2O_5 as a desiccant. Sample was evaluated for crystallinity after 2 ("day 3"), 4 ("day 5"), and 6 ("day 7") days of storage under dry conditions.

Based on the observations made, the samples were semi-quantitatively categorized at each time point as being (i) completely amorphous ("AAAA": no crystalline regions could be observed), (ii) slightly crystalline ("AAAC": crystallinity was observed, but amorphous regions dominated the sample), (iii) semi-crystalline ("AACC": the areas of crystalline and amorphous regions were comparable), (iv) predominantly crystalline ("ACCC": amorphous regions were observed, but crystalline material dominated the sample), or (v) completely crystalline ("CCCC": no amorphous regions could be observed). Based on the categorization of the crystallinity of the spin-coated samples at the different time points, the crystallization behavior

of the drug–solvent combinations was classified as being a rapid ("Class I": crystallinity on day 0 is at least AACC), intermediate ("Class II": crystallinity on day 7 is at least AACC), or slow ("Class III": crystallinity on day 7 is AAAA or AAAC).

A similar evaluation was performed for the samples obtained by slow evaporation, with the adaptation that the "day 0" time point was taken after allowing the solvent to evaporate.

Comparison With Classification Results from Cooling from the Melt

The classification data generated in this study were compared with the melt classification results for the same compounds.[1] For the melt classification, the crystallization behavior was identified as being rapid ("Class I": recrystallization of the sample occurs during cooling at 20°C/min), intermediate ("Class II": recrystallization of the sample is observed during subsequent reheating at 10°C/min), or slow ("Class III": no crystallization observed during cooling and subsequent reheating of the sample). Each of the 93 classification results obtained upon spin coating was therefore compared to that obtained for the same compound upon cooling from the melt. Subsequently, samples were grouped by their classification based on both preparation methods (e.g., Class $I_{evaporation}$–Class II_{melt}). The relative prevalence of each group was calculated by dividing the number of cases in that group by 93 (the total number of samples) and expressed as a percentage.

Principal Component Analysis (PCA)

PCA was performed using SIMCA-P+ software, version 12.0.0.0 (Umetrics AB, Umeå, Sweden). The following physical and molecular properties of the molecules were used as the x variables in the model: melting point [T_m (K), onset], glass transition temperature [T_g (K), midpoint], heat of fusion [ΔH_{fus} ($J\,cm^{-3}$)], entropy of fusion [ΔS_{fus} ($J\,cm^{-3}\,K^{-1}$)], the free energy difference between the crystalline and amorphous states [ΔG_v ($J\,cm^{-3}$)], molecular weight [MW ($g\,mol^{-1}$)], and the number of rotatable bonds (#RB). The values for T_m, T_g, and ΔH_{fus} were determined by DSC, as described previously.[1] ΔS_{fus} was calculated using the above determined values and Eq. (1):

$$\Delta S_{fus} = \frac{\Delta H_{fus}}{T_m} \quad (1)$$

ΔG_v was predicted using the Hoffmann equation (Eq. 2), using a temperature of 293.15 K for T

$$\Delta G_v = -\frac{\Delta H_{fus}(T_m - T)T}{T_m^2} \quad (2)$$

All ΔH_{fus}, ΔS_{fus}, and ΔG_v values were expressed on a volume basis by multiplying the weight-based values by the crystalline density. The latter was taken either from the crystal structure (average values were calculated in cases multiple structures were found in the Cambridge Structural Database) or when no crystal structure was available, by helium pycnometry. Values for MW and #RB were determined with ChemAxon calculator plugins using MarvinSketch, version 5.2.0 (ChemAxon Kft., Budapest, Hungary). For the 16 molecules where no T_g's could be determined due to rapid crystallization and no literature values could be found, T_g values were predicted based on the T_g/T_m ratios of the 35 compounds for which T_g's were available (further details are provided elsewhere[1]). The data of the variables were centered (by subtracting the average) and scaled to unit variance. Components were extracted and their significance was evaluated using cross-validation. PCA models were generated for the complete data set of compounds as well as for each class of compounds. Compounds which were classified as both Class I and Class II or Class II and Class III, depending on the solvent system used were regarded as belonging to Class I or Class III, respectively.

RESULTS AND DISCUSSION

Spin Coating as a Miniaturized System for Rapid Solvent Evaporation

In this study, spin coating was used as a small-scale screening technique to study solidification and subsequent crystallization behavior of APIs upon rapid solvent evaporation. As this technique is not widely employed in the field of pharmaceutical sciences, the process will be first considered in greater detail. Spin coating consists of the deposition of a thin layer of an initially dissolved material onto a substrate of choice, by rapidly rotating the substrate. The process has different stages[23]: (i) deposition, (ii) spin-up, (iii) spin-off, and (iv) solvent evaporation. Deposition consists of the delivery of an excess of the liquid to be coated onto the surface; spin-up is the stage of covering or wetting the entire surface with excess liquid. In our set-up (the solutions were spread over the entire surface prior to spinning), both processes occur simultaneously. During spin-off, the excess liquid is removed from the surface by centrifugal force, leaving behind (at least for Newtonian liquids, uniform in viscosity) a film of nearly uniform thickness that tends to become even more uniform as it thins further. In the case of drug solutions, the thinning proceeds until the rheology of the remaining liquid turns solid-like. The evaporation stage consists of concentration of the drug on the substrate. While solvent evaporation occurs simultaneously with the other stages described, the effect of evaporation on film thinning and liquid flow tends to

be secondary until the final stages of spin-off. Ultimately, the evaporation of solvents from an immobile, virtually solidified film is the main process contributing to the final stage of spin coating.[23] For drug solidification, the evaporation stage is the most important. In this stage, solvent removal will result in a supersaturated solution in which crystal nucleation, followed by growth can occur. As both the solubility of the drug and evaporation rate of the solvent will depend on the solvent system, the point where the solution becomes supersaturated will also depend on the solvent system selected, as will the evolution of the viscosity of the solution upon further solvent removal. The fact that (i) the overall process of spin coating is rapid and (ii) the formation of thin films having a large contact area with air (relative to their volume) is favorable in terms of solvent evaporation kinetics should minimize the potential for nucleation and growth in the supersaturated solution phase. The above characteristics of the spin-coating process have some similarity to industrially relevant unit operations used for solvent evaporation such as spray drying, in contrast to processes where the solidification process is slower, for example, evaporation at room temperature or using rotary evaporation. The rapid drying and solidification kinetics, small amounts of compound needed, and favorable characteristics in terms of throughput make this technique ideally suited to conduct a screening study on the crystallization behavior of a comprehensive, structurally diverse set of compounds in three solvent systems of different polarities.

Determination of the Optimal Drug Concentration for Spin Coating and Identification of Feasible Drug–Solvent Combinations

In order to utilize spin coating, it is first necessary to determine the minimum solution concentration necessary to enable the formation of a uniform film of sufficient thickness so that polarized light microscopy can be used to assess the presence or absence of crystallinity. The properties of spin-coated films prepared from solutions containing different concentrations of felodipine were therefore evaluated. The latter was selected as the compound for method development since we have considerable experience with spin coating this substance and it is known that an amorphous film can be generated with this procedure. The average film thickness of the films as a function of initial felodipine concentration is shown in Figure 1. As expected, film thickness increases with initial solution concentration. At higher concentrations (>0.26 M), DCM leads to the formation of films that are significantly thicker compared to those prepared with the MIX (the film thickness for felodipine in EtOH could not be evaluated at the higher concentrations due to the lower solubility of

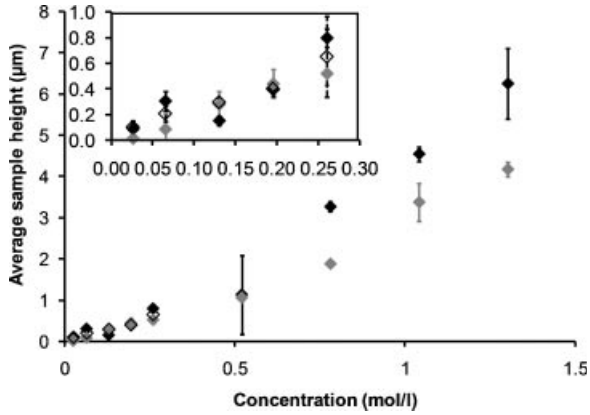

Figure 1. Average thickness of spin-coated films as a function of initial felodipine concentration in the solvents systems used in this screening. Key: black, DCM; gray, MIX; white, EtOH ($n = 3$).

felodipine in EtOH). This observation can most likely be explained by the higher volatility of DCM compared to EtOH; thus when using pure DCM, the point where the viscosity of the deposit limits its spin-off from the cover glass will be reached earlier, resulting in thicker films. At lower concentrations ($\leq$0.26 M, inset of Fig. 1), this effect cannot be seen, and films of similar average thickness are formed, irrespective of the solvent system applied. Furthermore, in the higher concentration range ($\geq$1.04 M), it could be visually observed that films were not flat, and polarized light microscopy revealed crystals in the bulk of the samples, suggesting both nonuniform deposition and slower solvent evaporation.

Photomicrographs obtained after allowing films of various thicknesses to crystallize under high relative humidity conditions are shown in Figure 2. As can be seen from the figure, crystals completely cover the surface of the sample when the films were prepared from solution concentrations $\geq$0.26 M. Below this concentration, drug coverage of the sample becomes incomplete, limiting crystallization. Similar behavior was seen using the other solvent systems (data not shown). Based on these observations, a workable concentration of 0.26–0.78 M was identified. To minimize the number of drop-outs, due to too low a solubility, the standard drug concentration for all spin-coating experiments was set at 0.26 M. Six drug–solvent combinations (anthranilic acid/DCM, celecoxib/DCM, felbinac/EtOH, miconazole/EtOH, nilutamide/MIX, probucol/EtOH), having a borderline solubility of 0.20–0.26 M, were included in the screening using a concentration of 0.20 M.

An additional requirement imposed was that no detectable degradation could be observed in the saturated drug solution used for solubility determination. The rationale for this criterion was based on the fact that drug degradation typically results in the formation of molecules having structures very similar

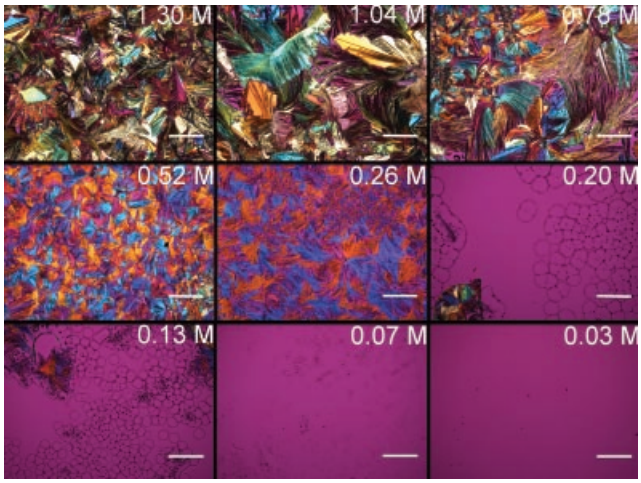

Figure 2. Polarized light microscopy of spin-coated felodipine films as a function of the initial concentration (prepared in DCM), after 2 days storage at 94% RH and room temperature. The bar represents 500 μm.

to that of the parent molecule, and it is well known that crystal nucleation and growth of organic molecules can be influenced by molecules having similar structures.[24–29] Molecules excluded from the screening because of degradation were griseofulvin, nifedipine, procaine, and tolfenamic acid.

Crystallization Behavior Following Spin Coating and upon Storage

After exclusion of various compounds due to low solubility, degradation, or sublimation, 93 drug–solvent combinations (40 compounds) were selected from the starting set of 153 combinations (51 compounds) for inclusion in the screening study. Table 2 provides an overview of the classification results based on the observed crystallization behavior of these 93 combinations (more detailed information, reporting the categorization at all time points can be found in the Supporting Information). From this set, 39 cases could be classified as Class I (rapid crystallization), 23 as Class II (intermediate crystallization), and 31 as Class III (slow crystallization). For Class I compounds, even with the very rapid solvent evaporation experienced by the sample during spin coating, extensive crystallization was observed immediately after spin coating, suggesting that these compounds have extremely fast nucleation and growth rates from supersaturated solutions or in the viscous film created during the later stages of solvent evaporation. Class II and Class III compounds could be produced as substantially amorphous films immediately following spin coating, but Class II compounds had a much higher tendency to crystallize over a relatively short (1 week) storage period at room temperature, whereas Class III compounds remained predominantly amorphous. Thus, Class II compounds have a higher tendency to crystallize from the amorphous film—this may be due either to the presence of nuclei formed during the spin-coating process, relatively rapid nucleation from the amorphous film, or a combination of both factors. Both of these mechanisms are probably important since about half of Class II compounds had a small amount of visible crystallinity following spin coating which would obviously act as seeds for additional crystallization, while the other compounds did not show evidence of any crystallinity until after a much later time period (see Supporting Information for more details). Clearly, the crystal growth rate from the amorphous film at room temperature in either instance was fast enough such that the amount of crystalline material formed was at least equal to the amorphous content after 1 week of storage. Class III compounds did not show any evidence of crystallinity immediately after spin

Table 2. Classification of the Crystallization Behavior of Samples Prepared by Spin Coating

Overall Class	Solvent System	DCM	MIX	EtOH
I	4-Biphenylcarboxylic acid		I	
	4-Biphenylmethanol	I	I	I
	4-Phenylphenol	I	I	I
	Anthranilic acid	I	I	I
	Benzamide	I	I	I
	Benzocaine	I	I	I
	Caffeine	I		
	Chlorzoxazone		I	I
	Dibucaine	I	I	I
	Felbinac		I	I
	Flufenamic acid	I	I	I
	Lidocaine	I	I	I
	Phenacetin	I	I	I
	Tolbutamide	I	I	I
I/II	Clofoctol	II	I	I
	Flurbiprofen	II	I	II
II	4-Biphenylcarboxaldehyde	II	II	II
	Bifonazole	II	II	
	Carbamazepine	II	II	
	Chlorpropamide	II	II	II
	Fenofibrate	II		
	Nilutamide	II	II	
	Nimesulide	II		
	Probucol	II		II
	Tolazamide	II		
II/III	Cinnarizine	II	III	
	Loratadine	III	II	II
III	Aceclofenac		III	
	Acetaminophen		III	III
	Atenolol		III	III
	Celecoxib	III	III	III
	Clotrimazole	III	III	III
	Felodipine	III	III	III
	Indomethacin	III	III	
	Itraconazole	III		
	Ketoconazole	III	III	
	Ketoprofen	III	III	III
	Miconazole	III	III	III
	Pimozide	III	III	
	Ritonavir	III	III	

Classes: Class I: rapid crystallization; Class II: intermediate crystallization; Class III: slow crystallization (see materials and methods section).

 DOI 10.1002/jps

coating (see Supporting Information) and showed a reduced tendency to crystallize over a 7-day storage period, implying slow nucleation and/or growth rates from the amorphous films.

It can also be seen from Table 2 that crystallization depends to a large extent on the compound studied and that the solvent system has only a small effect on the crystallization behavior. Only 10 out of the 33 compounds for which multiple solvents were evaluated (bifonazole, carbamazepine, celecoxib, cinnarizine, clofoctol, clotrimazole, felodipine, flurbiprofen, loratadine, and nilutamide) resulted in differences in the categorization at the various time points. Furthermore, these differences were typically subtle, resulting in a different classification for only four compounds (cinnarizine, clofoctol, flurbiprofen, and loratadine). While the effect of solvent selection on the solidification outcome is well recognized (e.g., polymorphic outcome[30]), it seems to be less critical in affecting if it is possible to form amorphous material as well as the subsequent physical stability of the amorphous solid, at least for the solvent systems and preparation method employed in this study. This can be explained by the very rapid solvent evaporation and fast film formation that occurs during spin coating, as described in the materials and methods section. Thus, any solvent-specific effect on nucleation and/or crystal growth is suppressed by the short time frame over which evaporation occurs.

To further illustrate this point, the crystallization behavior of the Class III compounds was investigated using conditions of slow evaporation. Data are provided in Table 3. Upon comparison of the obtained data with those from spin coating (see Supporting Information), it is clear that (i) it becomes harder to obtain amorphous material with slower evaporation rates (22 of the 31 drug–solvent combinations resulted in a "CCCC" categorization at the first time point) and (ii) in cases where crystallization is not complete at day 0 (clotrimazole, ketoprofen, miconazole, and ritonavir), the crystallization outcome becomes more variable, depending on the solvent used. The former observation is an obvious result of the longer time period where the solution experiences supersaturation during the evaporation stage prior to substantial increases in solution viscosity. The latter observation implies that the solvent has a much greater influence during the evaporation stage. The above results indicate that, using conditions of rapid solidification, the crystallization behavior of an API appears to be largely independent of the solvent system used. Therefore, two related questions arise: (i) to what extent is the crystallization tendency of the compounds upon solvent evaporation comparable to that during cooling/reheating from the melt and (ii) what physicochemical features of the molecule influence crystallization tendency?

Comparison of the Solvent and Melt Crystallization Classifications

The crystallization behavior of the compounds utilized in the current study also has been evaluated and classified upon cooling/reheating from the melt.[1] The crystallization behavior of the drugs was classified either as rapid (Class I: recrystallization of the sample occurs during cooling at 20°C/min), intermediate

Table 3. Crystallization of the Class III Samples Prepared by Slow Evaporation

	Solvent System														
	DCM					MIX					EtOH				
	Time Points														
	0	1	3	5	7	0	1	3	5	7	0	1	3	5	7
Aceclofenac						CCCC	CCCC	CCCC	CCCC	CCCC					
Acetaminophen						CCCC	CCCC	CCCC	CCCC	CCCC	CCCC	CCCC	CCCC	CCCC	CCCC
Atenolol						CCCC	CCCC	CCCC	CCCC	CCCC	CCCC	CCCC	CCCC	CCCC	CCCC
Celecoxib	CCCC	CCCC	CCCC	CCCC	CCCC	CCCC	CCCC	CCCC	CCCC	CCCC	CCCC	CCCC	CCCC	CCCC	CCCC
Cinnarizine						CCCC	CCCC	CCCC	CCCC	CCCC					
Clotrimazole	AAAC	AACC	AACC	AACC	ACCC	AAAC	AACC	AACC	ACCC	ACCC	AAAC	AAAC	AACC	AACC	AACC
Felodipine	CCCC	CCCC	CCCC	CCCC	CCCC	CCCC	CCCC	CCCC	CCCC	CCCC	CCCC	CCCC	CCCC	CCCC	CCCC
Indomethacin	CCCC	CCCC	CCCC	CCCC	CCCC	CCCC	CCCC	CCCC	CCCC	CCCC					
Itraconazole	CCCC	CCCC	CCCC	CCCC	CCCC										
Ketoconazole	CCCC	CCCC	CCCC	CCCC	CCCC	CCCC	CCCC	CCCC	CCCC	CCCC					
Ketoprofen	AAAA	AAAC	AAAC	AACC	AACC	AAAA	AAAA	AAAA	AAAA	AAAA	AAAA	AAAA	AAAA	AAAA	AAAA
Loratadine	CCCC	CCCC	CCCC	CCCC	CCCC										
Miconazole	CCCC	CCCC	CCCC	CCCC	CCCC	AAAA	AAAA	AAAA	AAAA	AAAA	AAAA	AAAA	AAAC	AAAC	AAAC
Pimozide	CCCC	CCCC	CCCC	CCCC	CCCC	CCCC	CCCC	CCCC	CCCC	CCCC					
Ritonavir	CCCC	CCCC	CCCC	CCCC	CCCC	AAAA	AAAA	AAAA	AAAC	AACC					

Categorization of the time points: AAAA: completely amorphous; AAAC: slightly crystalline; AACC: intermediately crystalline; ACCC: highly crystalline; CCCC: completely crystalline (see materials and methods section).

(Class II: recrystallization of the sample is observed during subsequent reheating at 10°C/min), or slow (Class III: no crystallization observed during cooling and subsequent reheating of the sample). Although the melt classification approach is somewhat different in that the influence of temperature perturbations over a short time scale on crystallization tendency is being evaluated rather than the crystallization tendency of samples upon rapid solvent evaporation followed by a more extended storage period at a fixed temperature, it is of interest to compare the crystallization behavior of the compounds under the two different assessment regimens. A comparison of the classification outcomes resulting from the two methods is provided in Table 4. From Table 4, it can be seen that identical classifications were obtained in 68% of the cases. Additionally, in 30% of the cases, the classification was only slightly different, that is, a Class II classification was obtained in one study while a more extreme classification (I or III) resulted from the other study. In only 2% of the cases and for only one compound (atenolol in MIX and EtOH), an extremely different crystallization outcome was observed (Class I according to the melt study and Class III by solvent evaporation). As it is clear that the way in which the classification criteria are defined will influence the resulting classification, it is of interest to compare the obtained results in greater detail. Of the 14 compounds yielding a Class I classification upon spin coating, 13 were classified in the same category upon cooling from the melt while only one (dibucaine) was classified as a Class II compound. Furthermore, of these 13 compounds, only 2 (flufenamic acid and tolbutamide) could be made amorphous if a faster cooling rate was used (i.e., quenching into liquid N_2), while no evidence of an amorphous phase could be found for the other 11 compounds (4-biphenylcarboxylic acid, 4-biphenylmethanol, 4-phenylphenol, anthranilic acid, benzamide, benzocaine, caffeine, chlorzoxazone, felbinac, lidocaine, and phenacetin). The two compounds classified either as Class I or Class II, depending on the solvent system used (clofoctol and flurbiprofen), were both Class II compounds according to the melt study. However, both tended to crystallize upon cooling if a slower cooling rate (1°C/min) was used. For the nine compounds falling into Class II upon spin coating, three were classified in the melt study as belonging to Class I (4-biphenylcarboxaldehyde, carbamazepine, and chlorpropamide), two as Class II (bifonazole and tolazamide), and four as Class III (fenofibrate, nilutamide, nimesulide, and probucol). Interestingly, all of the Class I compounds could be made amorphous upon quenching in liquid N_2. Furthermore, two of the four Class III compounds (nilutamide and nimesulide) were identified as the only Class III compounds that recrystallized using a slower heating rate of 2°C/min. The two compounds that yielded either Class II or Class III classifications, depending on the solvent system used, were classified according to the melt study either as a Class II (cinnarizine) or as Class III compound (loratadine). Of the 13 compounds classified as Class III compounds upon spin coating, melt classification yielded 1 Class I compound (atenolol), 2 Class II compounds (acetaminophen and celecoxib), and 10 Class III compounds (aceclofenac, clotrimazole, felodipine, indomethacin, itraconazole, ketoconazole, ketoprofen, miconazole, pimozide, and ritonavir). Atenolol was the only of the 40 compounds yielding an extremely different classification depending on the method of preparation used. Bearing in mind the different timescales of the two evaluation methods, plus the use of the melt versus a solution as the crystallization medium, the similarity in crystallization tendency of the various compounds is remarkable and has important practical implications. Thus, a drug which crystallizes readily during solvent evaporation (e.g., spray drying) would also be anticipated to crystallize easily from a melt state (e.g., melt extrusion). Clearly, this result is of relevance when considering the use of the amorphous form of the drug for the final dosage form. Furthermore, the similarity between crystallization outcomes between the two methods suggests that using conditions of rapid solidification, the crystallization tendency is dominated by the physicochemical properties of the API, with the solidification methodology being less important. Hence, it is of interest to try to understand some of the key API properties influencing the crystallization outcome.

Influence of Physicochemical Compound Characteristics on Crystallization Behavior

As discussed above, for APIs falling into the extreme classes of crystallization behavior (i.e., Class I and Class III), it appears to be the compound rather than

Table 4. Comparison of Classification Results Obtained after Solvent Evaporation by Spin Coating With Those Obtained upon Cooling from the Melt by DSC

	Class I_{melt} (%)	Class II_{melt} (%)	Class III_{melt} (%)	Totals
Class $I_{evaporation}$ (%)	35	6	0	42
Class $II_{evaporation}$ (%)	9	8	9	25
Class $III_{evaporation}$ (%)	2	6	25	33
Totals (%)	46	20	33	100

Percentages represent the number of drug–solvent combinations, divided by 93 (the total number of drug–solvent combinations).

the processing conditions that tends to determine the crystallization behavior. Given the complex nature of crystallization, a multivariate approach seemed to be the most appropriate method to evaluate the importance of various factors to the crystallization outcome. Therefore, principle component analysis (PCA) was performed using various thermal (T_m, T_g, ΔH_{fus}, ΔS_{fus}, ΔG_v), and molecular [MW, number of rotatable bonds (#RB)] input parameters for the set of 40 molecules. It should be noted that no information about the class of compound was used to generate the PCA model. A PCA model was generated with three principal components. This model could explain 97.6% of the variation in the input parameters (55.9%, 30.7%, and 11.0% by the 1st, 2nd, and 3rd components, respectively). Cross-validation indicated that 89.8% of the variation could be predicted (31.3% and 69.5% for models with only the 1st and the 1st and 2nd components), indicating good predictivity. The scores plot for the 1st and 2nd components is shown in Figure 3. Each data point represents a single compound and has been shaded according to compound class. Compounds for which different solvents yielded different classifications were regarded as belonging either to Class I or Class III (and not to Class II). It is apparent from Figure 3 that Class I compounds tend to populate the left and lower sides of the plot, while Class III compounds dominate the upper right side of the plot, although some exceptions can be observed. Class II compounds are more scattered across the plot. Thus, the 1st and 2nd components enable a certain extent of differentiation between the different classes, based only on the input parameters described above. The 3rd component did not contribute to discrimination between the classes (data not shown). To further investigate how the physicochemical properties of the compounds differ between classes, class contributions were determined. The contributions (Fig. 4, not weighted) indicate how the average values of the descriptors for the different classes differ from the averages obtained from the complete set of compounds. It can be seen from Figure 4 that molecular weight and number of rotatable bonds tend to be higher for Class III and lower for Class I compounds. For crystallization to occur, molecules have to become correctly orientated into the crystal lattice. Hence, the observation that molecules with more complex and flexible structures have a lower crystallization tendency is both intuitive and in line with earlier observations.[1,31] The enthalpy and entropy of fusion are higher for Class I molecules and lower for Class II and Class III molecules. Consequently, the estimated crystalline–liquid free energy difference is more negative for Class I molecules. According to classical nucleation theory,[32,33] an increased free energy change for the crystalline transformation on a per unit volume basis, ΔG_v, will lead to a reduced nucleation barrier as shown by Equation 3:

$$W^* = \frac{16\pi\gamma^3}{3\Delta G_v^2} \quad (3)$$

where W^* is the free energy change on formation of a nucleus of a critical size, and γ is the interfacial free energy per unit of area at the nucleus–liquid interface. The nucleus–liquid interface denotes either the developing crystal surface and the highly supersaturated solution or the crystalline surface and the supercooled liquid/glass, depending on which stage in the solidification process crystallization takes place (i.e., before or after solvent

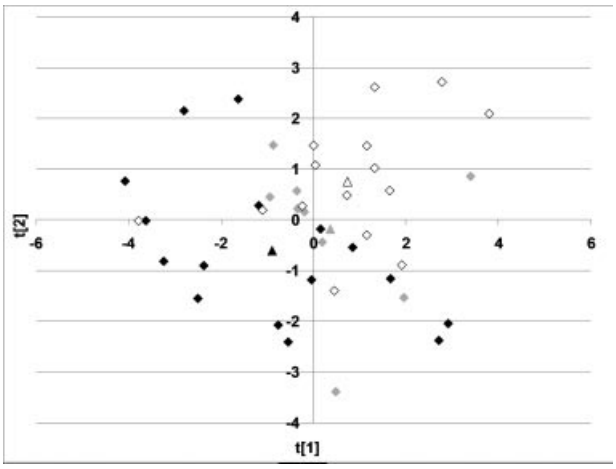

Figure 3. Scores plot of the PCA model (1st and 2nd components), shaded according to class. Key: black, Class I; gray, Class II; white, Class III. Diamonds represent the individual compounds, and triangles are the averages of the different classes. In cases where different classifications were obtained using different solvents (Class I/II or Class II/III), the compound was classified as being either Class I or Class III.

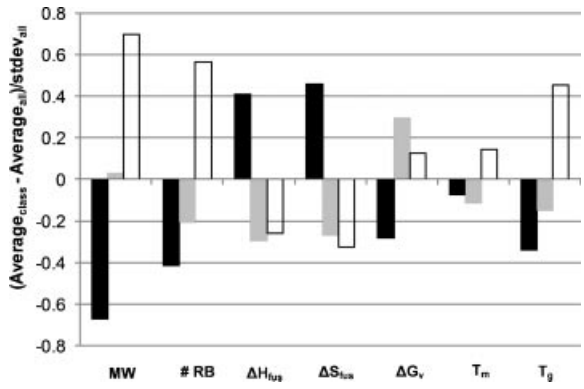

Figure 4. Contribution plots for the different classes (not weighted). Key: black, Class I; gray, Class II; white, Class III.

evaporation) and the T_g of the system relative to room temperature. Although W^* depends to the 3rd power on γ while only to the 2nd power on ΔG_v, our observations of the correlation between ΔG_v and crystallization tendency are consistent with theory. While γ values are difficult to either measure or estimate, the observed correlation with ΔG_v suggests that γ differences between systems are small compared to those seen for ΔG_v.

While all of the above differences between Class I and Class III compounds could also be observed in the melt,[1] T_m and T_g show different trends in terms of their correlation with crystallization outcome for the two preparation methods. For melt crystallization, some differences were seen for the average values of T_m between the classes; however, only minor differences can be observed between Class I and Class III compounds upon spin coating. For T_g, on the other hand, it can be seen that solvent Class I (and Class II) compounds tend to have lower values, while Class III compounds have higher values (little discrimination between T_g values for the different melt classes was observed). This difference can be readily understood by considering that Class III compounds fail to crystallize to any substantial extent following storage for several days at room temperature. This classification criterion will tend to select for compounds that have a higher T_g and are therefore in the glassy state at the storage temperature. In contrast, the melt classification procedure investigates the crystallization behavior over a much shorter timeframes with all samples being exposed to temperatures above T_g.

A final question to address is to what extent the crystallization behavior of compounds can be predicted based on their physicochemical characteristics? To evaluate this, individual PCA models were built for each of the classes. For each class, a three-component model was generated (Class I: 97.9% of variability explained, 87.9% predictable; Class II: 99.1% of variability explained, 88.1% predictable; Class III: 96.1% of variability explained, 76.7% predictable). A Coomans' plot of the models for Class I and Class II is provided in Figure 5. This type of plot evaluates how well predictions fit into two PCA models, by calculating the distance to both models (DModXPS+). The lines in the plot represent the critical distance to the model (significance level 0.05). Hence, the lower the distance to a model the better that compound fits that model. As all compounds showed small distances to the model generated for the Class III compounds (data not shown), the latter has very limited discriminative potential and was not used further. From the Coomans' plot of the Class I and Class II models, the following observations can be made: First, it can be seen that generally (although not always), Class III compounds show

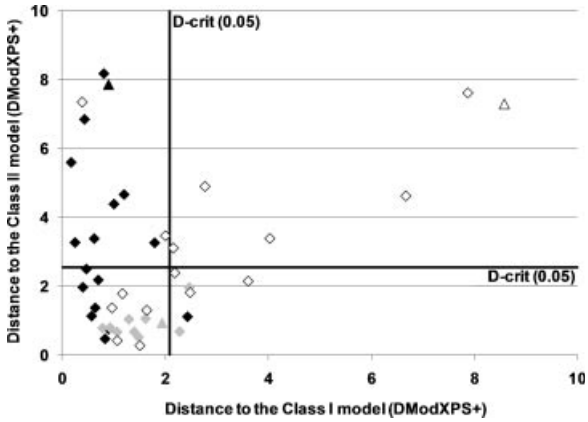

Figure 5. Coomans' plot for the Class I and Class II models. Key: white, Class I; gray, Class II; black, Class III. Diamonds represent the individual compounds, and triangles are the validation compounds used to assess predictivity (Class I: PABA; Class II: piroxicam; Class II: clarithromycin). The lines in the plot represent the critical distance to the model (significance level 0.05).

large distances to both models. Second, Class I compounds frequently show large distances to the model of the Class II compounds. Third, although the Class II compounds are characterized by small distances to the Class I model, they all tend to be located in a very small region of the Cooman's plot. Based on the above observations, some predictivity potential can be expected using this type of analysis. To further validate this, distances to the Class I and Class II models were determined for three additional compounds (not used to build the models), one of each class [Class I: PABA (MIX and EtOH); Class II: piroxicam (DCM), Class III: clarithromycin (DCM)]. As can be seen from Figure 5 where the triangles represent these additional samples, the crystallization behavior of both the Class I and Class III validation compounds was well predicted from the physicochemical input parameters. The distances to the models observed for the Class II validation compound suggest a potential Class II behavior, although other classifications might also be possible.

Summarizing, the process of crystallization is complex and consideration of a single descriptor cannot be used to understand crystallization behavior upon solvent evaporation. However, as for cooling from the melt, differences could be observed in the average values of the descriptors for the different classes, which could be further interpreted in terms of the crystallization process. Furthermore, using a number of easily accessible descriptors to construct an appropriate PCA model, a first pass *a priori* evaluation of the crystallization tendency of a compound can be made.

 DOI 10.1002/jps

CONCLUSIONS

Spin coating of drug solutions proved to be a useful, low consumption technique for the preparation of thin films of drugs and the subsequent screening of crystallization tendency. Upon monitoring the crystallization behavior of the films following spin coating, clear differences could be observed between different drugs. Based on their crystallization behavior, drug–solvent combinations could be classified as rapid (Class I), intermediate (Class II), or slow (Class III) crystallizers. PCA of the data set, using various molecular and thermal descriptors as input parameters, indicated that score values for Class I and Class III compounds tend to differ. This result suggests that, with a suitable data set, PCA analysis may provide some *a priori* prediction of crystallization tendency if a few simple compounds properties are known. Interestingly, good correlations were noted between crystallization tendency upon rapid solvent evaporation and upon cooling from the melt. This important observation suggests that under conditions of rapid solidification, crystallization is governed mainly by the inherent properties of the compound. Thus, in terms of physical stability, Class I compounds will be much more challenging to maintain as the amorphous form compared to Class III compounds. Therefore, they may not be appropriate candidates for solid dispersion technology.

ACKNOWLEDGMENTS

The authors would like to thank the National Science Foundation Engineering Research Center for Structured Organic Particulate Systems for financial support (NSF ERC-SOPS) (EEC-0540855).

REFERENCES

1. Baird JA, Van Eerdenbrugh B, Taylor LS. 2010. A classification system to assess the crystallization tendency of organic molecules from undercooled melts. J Pharm Sci DOI: 10.1002/jps.22197.
2. Amidon GL, Lennernäs H, Shah VP, Crison JR. 1995. A theoretical basis for a biopharmaceutic drug classification—The correlation of in-vitro drug product dissolution and in-vivo bioavailability. Pharm Res 12:413–420.
3. Rabinow BE. 2004. Nanosuspensions in drug delivery. Nat Rev Drug Discov 3:785–796.
4. Brewster ME, Loftsson T. 2007. Cyclodextrins as pharmaceutical solubilizers. Adv Drug Deliv Rev 59:645–666.
5. Millard JW, Alvarez-Núñez FA, Yalkowsky SH. 2002. Solubilization by cosolvents—Establishing useful constants for the log-linear model. Int J Pharm 245:153–166.
6. Stella VJ, Nti-Addae KW. 2007. Prodrug strategies to overcome poor water solubility. Adv Drug Deliv Rev 59:677–694.
7. Leuner C, Dressman J. 2000. Improving drug solubility for oral delivery using solid dispersions. Eur J Pharm Biopharm 50:47–60.
8. Hancock BC, Parks M. 2000. What is the true solubility advantage for amorphous pharmaceuticals? Pharm Res 17:397–404.
9. Ambike AA, Mahadik KR, Paradkar A. 2004. Stability study of amorphous valdecoxib. Int J Pharm 282:151–162.
10. Gupta P, Kakumanu VK, Bansal AK. 2004. Stability and solubility of celecoxib-PVP amorphous dispersions: A molecular perspective. Pharm Res 21:1762–1769.
11. Van Eerdenbrugh B, Van Speybroeck M, Mols R, Houthoofd K, Martens JA, Froyen L, Van Humbeeck J, Augustijns P, Van den Mooter G. 2009. Itraconazole/TPGS/Aerosil® 200 solid dispersions: Characterization, physical stability and in vivo performance. Eur J Pharm Sci 38:270–278.
12. van Drooge DJ, Hinrichs WLJ, Frijlink HW. 2004. Anomalous dissolution behavior of tablets prepared from sugar glass-based solid dispersions. J Control Release 97:441–452.
13. Savolainen M, Kogermann K, Heinz A, Aaltonen J, Peltonen L, Strachan C, Yliruusi J. 2009. Better understanding of dissolution behaviour of amorphous drugs by in-situ solid-state analysis using Raman spectroscopy. Eur J Pharm Biopharm 71: 71–79.
14. Alonzo DE, Zhang GGZ, Zhou D, Gao Y, Taylor LS. 2010. Understanding the behavior of amorphous pharmaceutical systems during dissolution. Pharm Res 27:608–618.
15. Bhugra C, Pikal MJ. 2008. Role of thermodynamic, molecular, and kinetic factors in crystallization from the amorphous state. J Pharm Sci 97:1329–1349.
16. Hancock BC, Zografi G. 1997. Characteristics and significance of the amorphous state in pharmaceutical systems. J Pharm Sci 86:1–12.
17. Willart JF, Descamps M. 2008. Solid state amorphization of pharmaceuticals. Mol Pharm 5:905–920.
18. Ravis WR, Chen CY. 1981. Dissolution, stability, and absorption characteristics of dicumarol in polyethylene glycol-4000 solid dispersions. J Pharm Sci 70:1353–1357.
19. Six K, Verreck G, Peeters J, Brewster M, Van den Mooter G. 2004. Increased physical stability and improved dissolution properties of itraconazole, a class II drug, by solid dispersions that combine fast- and slow-dissolving polymers. J Pharm Sci 93:124–131.
20. Marsac PJ, Konno H, Taylor LS. 2006. A comparison of the physical stability of amorphous felodipine and nifedipine systems. Pharm Res 23:2306–2316.
21. Greaser KA, Patterson JE, Zeitler JA, Gorond KC, Rades T. 2009. Correlating thermodynamic and kinetic parameters with amorphous stability. Eur J Pharm Sci 37:492–498.
22. Marsac PJ, Shamblin SL, Taylor LS. 2006. Theoretical and practical approaches for prediction of drug-polymer miscibility and solubility. Pharm Res 23:2417–2426.
23. Bornside DE, Macosko CW, Scriven LE. 1987. On the modeling of spin coating. J Imaging Technol 13:122–130.
24. Hendriksen BA, Grant DJW. 1995. The effect of structurally related substances on the nucleation kinetics of paracetamol (acetaminophen). J Cryst Growth 156:252–260.
25. Lechuga-Ballesteros D, Rodríguez-Hornedo N. 1995. The influence of additives on the growth-kinetics and mechanism of L-alanine crystals. Int J Pharm 115:139–149.
26. Davey RJ, Blagden N, Potts GD, Docherty R. 1997. Polymorphism in molecular crystals: Stabilization of a metastable form by conformational mimicry. J Am Chem Soc 119:1767–1772.
27. Hendriksen BA, Grant DJW, Meenan P, Green DA. 1998. Crystallisation of paracetamol (acetaminophen) in the presence of structurally related substances. J Cryst Growth 183:629–640.

28. Weissbuch I, Lahav M, Leiserowitz L. 2003. Toward stereochemical control, monitoring, and understanding of crystal nucleation. Cryst Growth Des 3:125–150.
29. Anwar J, Boateng PK, Tamaki R, Odedra S. 2009. Mode of action and design rules for additives that modulate crystal nucleation. Angew Chem Int Ed 48:1596–1600.
30. Khoshkhoo S, Anwar J. 1993. Crystallization of polymorphs: The effect of solvent. J Phys D Appl Phys 26:B90–B93.
31. Yu L, Reutzel-Edens SM, Mitchell CA. 2000. Crystallization and polymorphism of conformationally flexible molecules: Problems, patterns, and strategies. Org Process Res Dev 4:396–402.
32. Turnbull D, Fisher JC. 1949. Rate of nucleation in condensed systems. J Chem Phys 17:71–73.
33. James PF. 1985. Kinetics of crystal nucleation in silicate-glasses. J Non-Crystalline Solids 73:517–540.

 DOI 10.1002/jps